Available online at www.sciencedirect.com
ScienceDirect
Ceramics International 36 (2010) 2189–2196
CERAMICS INTERNATIONAL
www.elsevier.com/locate/ceramint

State dependent pyroelectric and thermal expansion coefficients in a PZT wafer

Sang-Joo Kim [a,*], Yong Soo Kim [b,1]

[a] Department of Mechanical and Information Engineering, University of Seoul, Dongdaemun-gu, Seoul 130-743, Republic of Korea
[b] Defense Agency for Technology and Quality, Cheongryang PO Box 276, Dongdaemun-gu, Seoul 130-650, Republic of Korea

Received 10 February 2010; received in revised form 19 April 2010; accepted 7 May 2010
Available online 23 June 2010

Abstract

A PZT wafer is subjected to a temperature increase from the reference temperature 20–111 °C under no electric field. During the temperature increase, the variations of remanent polarization in thickness direction and remanent in-plane strain are measured. From the measurements, the values of pyroelectric coefficient in thickness direction and in-plane thermal expansion coefficient are estimated. The temperature experiment is repeated starting at various different values of initial remanent polarization, and the dependency of pyroelectric and thermal expansion coefficients on initial remanent polarization is obtained. In the tested range of temperature, it is found that the pyroelectric coefficient can be given as a linear function of remanent polarization and that the in-plane thermal expansion coefficient is given as a linear function of remanent in-plane strain or as a quadratic function of remanent polarization.

Keywords: Thermal expansion; PZT wafer; Temperature; Switching; Pyroelectric

1. Introduction

Lead zirconate titanate (PZT) ceramics have been widely used in the fields of actuators and sensors. These ferroelectric materials have several beneficial properties such as large generative force, quick response time, low power consumption, relatively high Curie temperatures and relatively low sintering temperatures. In these applications, it is important to predict the performance or reliability of the piezoelectric devices. The predictions are usually made by finite element methods, which require a reliable constitutive model for the linear and nonlinear behavior of the materials. The constitutive models for finite element analyses are often developed based on macro-state variables such as remanent polarization and remanent strain. Thus the knowledge of the dependence of material linear moduli on remanent quantities is important for the construction of a reliable constitutive model. The researches done by Selten et al. [1] and Liu and Huber [2] are the examples of the efforts describing linear moduli as functions of remanent quantities at room temperature. They observed the dependence of permittivity, piezoelectric coefficients, and elastic moduli on remanent polarization under electric fields and/or compressive stress loads. Experimental observations on nonlinear creep behavior of the materials under electric fields have also been made by Zhou and Kamlah [3], Liu and Huber [4], and Kim and Lee [5], which may be helpful in the modeling of the materials. However, their studies are all limited to room temperature. Considering that some piezo actuators are used in the environments with a wide range of temperature due to either the change in ambient temperature or a high temperature generated by the self-heating of the dissipative materials. A temperature increase more than 75 °C was observed during an operation of a piezoelectric stack actuator at 130 Hz driving frequency at a surrounding temperature of 120 °C, which is shown to deteriorate the function of the actuator by depolarization, see Sakai and Kawamoto [6]. Therefore, the efforts of constructing a constitutive model of ferroelectric ceramics should be extended to high temperatures.

Recently, Kim et al. [7,8] investigated time-dependent behavior of a poled PZT wafer under constant magnitudes of through thickness electric fields at high temperatures. In order

* Corresponding author. Tel.: +82 2 2210 2757; fax: +82 2 2210 5575.
E-mail address: sangjookim@gmail.com (S.-J. Kim).
[1] Tel.: +82 2 2079 1131; fax: +82 2 779 4879.

0272-8842/$36.00
doi:10.1016/j.ceramint.2010.05.026

to compare domain switching processes at different high temperatures, they measured pyroelectric and thermal expansion coefficients by increasing the temperature of the wafer under no electric field. However, since the material properties were measured at a poled state only, their dependency on remanent polarization and strain was not clearly understood yet. In the present work, the pure temperature experiments are made at various initial values of remanent polarization at the reference temperature 20 °C. The effects of the directions of the electric field used to obtain the initial reference remanent polarization are also examined experimentally. Plotting, fitting, and analyzing the measured data, the pyroelectric and thermal expansion coefficients could be expressed approximately as functions of remanent polarization, remanent in-plane strain, and temperature.

2. Experimental

A commercially available soft wafer (3203HD, CTS, USA) of dimensions 71 mm × 23 mm × 0.5 mm with the Curie point 225 °C was used for experiments. The longitudinal, transverse and thickness directions of the wafer are designated as x_1, x_2 and x_3 and are often called as 1, 2 and 3 directions, respectively, through the whole paper. It is usually assumed that the internal domain structure of a PZT wafer poled in thickness direction can be described by two macroscopic quantities: remanent through thickness polarization P_3^R and remanent in-plane strain ε_1^R. In the present work, the variations of P_3^R and ε_1^R in a PZT wafer are measured when temperature is increased from the reference temperature $\theta_0 = 20$ °C to 110 °C. The values of P_3^R and ε_1^R at reference temperature θ_0 are denoted as P_3^{R0} and ε_1^{R0}, respectively, and they are called reference remanent polarization and reference remanent strain, respectively. In order to see the dependency of material thermal properties on remanent state variables, a PZT wafer that is poled initially in the $-x_3$ direction is subjected to a constant magnitude of through thickness electric field in the $+x_3$ direction for a short period of time at the reference temperature $\theta_0 = 20$ °C, as shown in Fig. 1(a). Then domain switching occurs in the $+x_3$ direction and the value of P_3^{R0} increases with the electric field loading. Reaching an initial value of P_3^{R0} for temperature experiment, the electric field loading is stopped. Then, after about 10 min for stabilization, the temperature of the wafer is increased from the reference temperature $\theta_0 = 20$ °C to 110 °C under no external electric field, and the two remanent quantities P_3^R and ε_1^R are measured. The measured variations of P_3^R and ε_1^R during the temperature increase correspond to the internal state represented by the initial values of P_3^{R0} and ε_1^{R0} at $\theta = \theta_0$. To obtain the evolutions of P_3^R and ε_1^R at other initial states of P_3^{R0} and ε_1^{R0}, temperature is decreased down to θ_0 and the wafer specimen is subjected to an initialization process in the $-x_3$ direction, to recover the original negatively poled state. During the initialization process, the specimen is subjected to a constant electric field of -0.9 MV m^{-1} for 1000 s. Then, after a sufficient time of zero field, an in-plane strain was measured and it was found to be less than about 30×10^{-6}, which is just 3% of the maximum in-plane strain obtained during an electric field loading. This shows that the specimen state obtained by the initialization process is sufficiently close to the original poled state, justifying the repeated use of the same specimen wafer for other temperature experiments. For next experiment, the wafer is subjected to another constant positive electric field to obtain a different value of P_3^{R0}. After reaching the different internal state represented by different values of P_3^{R0}, the temperature of the wafer is increased and P_3^R and ε_1^R are measured, which is exactly the same as the previous experiment. Similar procedures are taken again and again, and the evolutions of P_3^R and ε_1^R at various values of P_3^{R0} are measured. In the present paper, a total of thirteen temperature experiments were made at the values of $P_3^{R0} = -0.298$, -0.228, -0.169, -0.12, -0.088, -0.049, -0.005, -0.005, 0.046, 0.116, 0.166, 0.208, 0.28, and 0.29 C m^{-2}, which are all obtained by applying positive electric fields to a negatively poled wafer, as shown in Fig. 1(a).

In the temperature experiments mentioned above, the initial internal state represented by P_3^{R0} was obtained by applying a positive electric field to a negatively poled wafer. Now, in order to clearly see the dependency of thermal material properties on remanent state variables, the initial internal state for temperature experiment is obtained by applying a negative electric field to a positively poled wafer, as shown in Fig. 1(b). In this case, a wafer is poled in the $+x_3$ direction by an initialization process. Then a negative electric field is used to obtain the value of P_3^{R0} for temperature experiment. After reaching the specific value of P_3^{R0}, temperature is increased under no electric field, and P_3^R and ε_1^R are measured. Repeating similar procedures, the evolutions of P_3^R and ε_1^R are obtained at various values of P_3^{R0}. In the present work, a total of thirteen measurements are made at $P_3^{R0} = -0.32$, -0.246, -0.22, -0.18, -0.165, -0.11, -0.087, 0.015, 0.048, 0.076, 0.15, 0.266 and 0.317 C m^{-2}, which are obtained by applying negative electric fields to the positively poled wafer specimen, as in Fig. 1(b).

During the whole experiments of electric field loading and subsequent temperature change, the wafer remains isotropic with respect to the thickness direction of the wafer and thus the longitudinal stain of the wafer is numerically equal to the transverse strain. The longitudinal and transverse strains in the

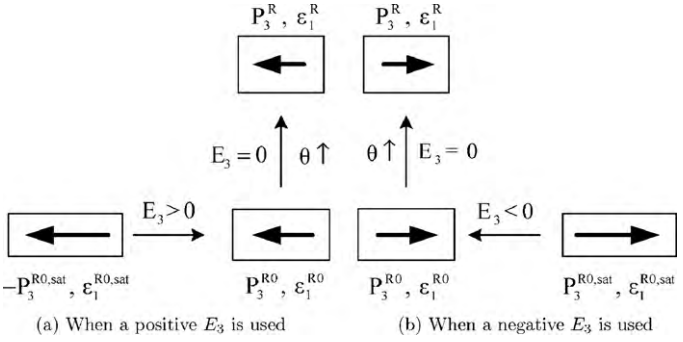

Fig. 1. Two methods to reach the initial state P_3^{R0} and ε_1^{R0} for temperature experiments: (a) a positive electric field is used and (b) a negative electric field is used. Then temperature is increased from 20 °C to 110 °C at a rate of 0.5 °C/min under no electric field.

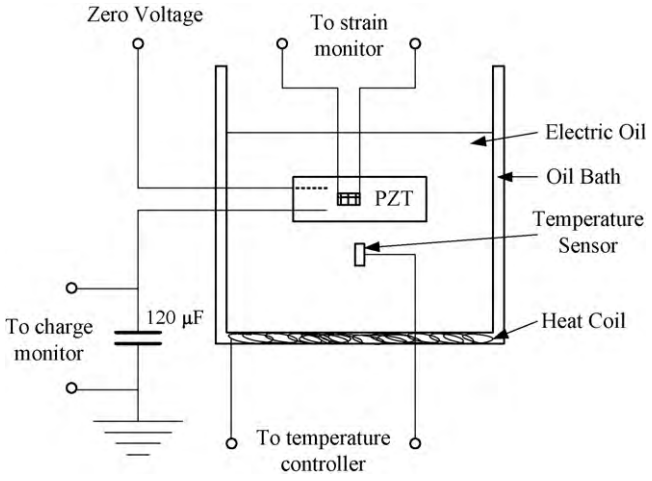

Fig. 2. Schematic diagram of a poled PZT wafer subjected to electric field loading and subsequent temperature increase for measuring in-plane strain and electric displacement in thickness direction.

plane of the wafer are measured from two strain gauges attached on both sides of the wafer, two in-plane strain components from each strain gauge. The four strain components are averaged to give the extensional strain component in the plane of the wafer. In the present paper, the extensional strain component in the plane of the wafer is called as an in-plane strain and it is denoted as ε_1. The strain gauges used to measure the in-plane strain are fully encapsulated constantan strain gauges (WA-03-062TT-350, VISHAY, Germany), whose measurements are reliable in the temperature range between −75 °C and 205 °C owing to a temperature compensation curve provided by the manufacturer. In addition, the strain gauges were verified by measuring the thermal strains of an aluminum wafer at high temperatures. In order to control the temperature of a specimen wafer, it is immersed into a bath of transformer oil (MICTRANS Class1-No2, MICHANG OIL IND. Co., Pusan, Korea) and the temperature of the oil is controlled using an electric heat coil located in the bottom plate of the bath and a temperature control unit (2408 PID controller, EUROTHERM, UK), as shown in Fig. 2. The measurements of the electric displacement in thickness direction were made by a Sawyer-Tower bridge. In the Sawyer-Tower circuit, a reference capacitor (metalized polypropylene capacitor) of capacitance 120 μF is connected to the specimen in series, which is 1200 times larger than the specimen capacitance 0.1 μF. The voltage across the reference capacitor was measured by a Keithley 6514 electrometer. Discharge circuits were added to the system to remove the charges accumulated in the specimen and the reference capacitor during experiments. All equipment output signals passed through a data acquisition board (PCI 6221, National Instruments, TX, USA) and are manipulated using a LABVIEW software.

3. Results and discussion

The measured remanent polarization in thickness direction P_3^R and remanent in-plane strain ε_1^R during pure temperature increase are shown in Fig. 3. As explained before, two methods are used to obtain the initial states at which temperature starts to increase. The initial states for measurements in Fig. 3(a) are obtained by applying positive electric fields to a negatively poled wafer and those in Fig. 3(b) by applying negative electric fields to a positively poled wafer. Only typical six among the total thirteen measurements in each loading case are drawn in the figures. The values of P_3^{R0} corresponding to the chosen six initial states are written in the figures. The upper figures show the evolutions of P_3^R and the lower ones the evolutions of ε_1^R over temperature. It is shown that both P_3^R and ε_1^R change linearly with temperature in the tested range of temperature.

It is interesting to see the relation of P_3^R and ε_1^R during temperature increase at various initial states, as shown in Fig. 4. The same data as in Fig. 3 were used for the graphs in Fig. 4. Fig. 4(a) shows the ε_1^R versus P_3^R graphs at various values of P_3^{R0}, which are obtained by applying a positive electric field to a negatively poled wafer; Fig. 4(b) shows the same graphs when a negative electric field is applied to a positively poled wafer. As expected, the graphs in Fig. 4(a) are symmetric with those in Fig. 4(b), due to the symmetry of material structure and electric field loading. The upper plots in Fig. 4 show the evolutions of P_3^R and ε_1^R at the same initial state, that is, at the same value of P_3^{R0}; the lower plots show the relations between P_3^R and ε_1^R at the same temperature. It is clearly seen in Fig. 4 that the ε_1^R versus P_3^R graphs for a positive electric field case are symmetric with those for a negative electric field case. The variations of ε_1^R over P_3^R are not symmetric with respect to zero polarization vertical line at all four temperatures, in both cases of electric field loading. Maximum remanent in-plane strain occurs at about $P_3^R = -0.1\,\mathrm{C\,m^{-2}}$ for positive electric field case in Fig. 4(a) and at about $P_3^R = +0.1\,\mathrm{C\,m^{-2}}$ for negative electric field case in Fig. 4(b).

The variations of P_3^R during a pure temperature increase shown in the upper plots of Fig. 3 can be fitted into straight lines. This means that the rate of change in P_3^R over temperature is constant in the temperature range between 20 °C and 110 °C. The slopes of the straight lines are equal to the values of pyroelectric coefficient p_3^σ at constant stress. The value of p_3^σ, therefore, remains constant in the temperature range between 20 °C and 110 °C. After getting the values of p_3^σ at various values of P_3^{R0}, it is interesting to see the dependency of p_3^σ on remanent polarization P_3^R at 20 °C. Fig. 5(a) shows the variations of p_3^σ over P_3^R at the reference temperature 20 °C, for both positive and negative electric field cases. The plotted data are well fitted by straight lines for both positive and negative electric field cases. The two fitted straight lines in Fig. 5(a) are almost parallel to each other. It is interesting that the value of p_3^σ at $P_3^R = 0$ is below zero for positive electric field case and it is above zero by the same amount for positive field case. However, it is natural to expect that the value of P_3^R remains zero, that is, $p_3^\sigma = 0$, if temperature is increased initially at $P_3^{R0} = 0$ and domain switching does not occur during the temperature increase. Thus, a nonzero value of p_3^σ at $P_3^R = 0$ in Fig. 5(a) means that domain switching does occur during the pure temperature increase. The negative value of p_3^σ at $P_3^R = 0$ for positive electric field case indicates that domain switching occurs in the negative $-x_3$ direction; the positive value of p_3^σ at

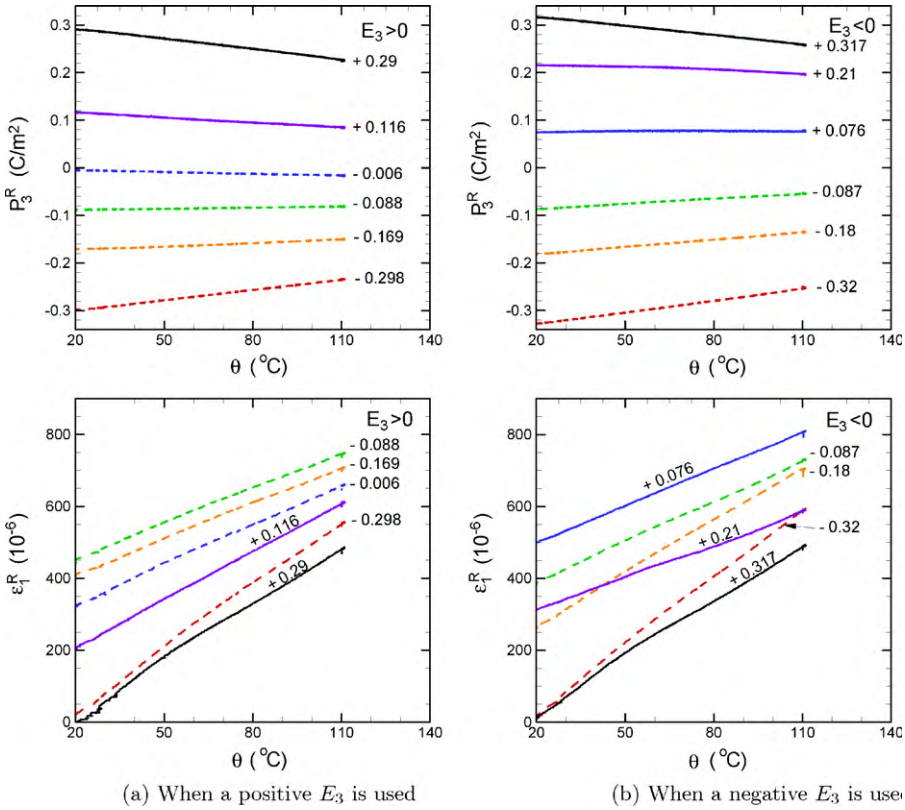

Fig. 3. Evolutions of remanent through thickness polarization P_3^R (upper plots) and remanent in-plane strain ε_1^R (lower plots) when temperature is increased from 20 °C to 110 °C under no electric field. The numbers in the figure represent the values of P_3^{R0} at which temperature starts to increase. The various values of P_3^{R0} were obtained by applying (a) a positive electric field to a negatively poled wafer or (b) a negative electric field to a positively poled wafer.

$P_3^R = 0$ for negative electric field case indicates that switching occurs in the positive $+x_3$ direction. Domain switching occurs in the direction opposite to the direction of electric field used to obtain the initial state for the temperature experiment. The difference of p_3^σ at $P_3^R = 0$ for the two cases of $E_3 > 0$ and $E_3 < 0$, therefore, is due to domain switching of opposite directions. It looks that the magnitude of difference in p_3^σ at $P_3^R = 0$ remains the same for all other values of P_3^R, meaning the same amount of domain switching occurs in the temperature experiments starting at other initial states of P_3^R.

Turning to in-plane thermal expansion coefficient α_1^E, Fig. 5(b) shows the variations of α_1^E at various initial states of P_3^R at 20 °C for both cases of electric field loading directions. The plotted data are well fitted by polynomial curves of third order. Maximum values of α_1^E are obtained at the negative or positive poled states, whereas the locations of minimum α_1^E depend on how the initial states P_3^{R0} are obtained. When a positive (or negative) electric field was used to reach the initial state represented by P_3^{R0}, the minimum α_1^E occurs at about $-0.1\ \mathrm{C\,m^{-2}}$ (or $+0.1\ \mathrm{C\,m^{-2}}$). Approximately, the fitted third order curve for a positive electric field is symmetric with the curve for a negative electric field.

It has been reported that the length of a ferroelectric tetragonal lattice decreases in the crystallographic c direction but it increases in the crystallographic a direction during a temperature rise, for example, see Jona and Shirane [9]. Therefore, the value of the thermal expansion coefficient in the plane of the wafer α_1^E at constant electric field depends on the ratio of the amounts of the variants in the in-plane directions of the wafer over those in the thickness direction of the wafer. This means that we may predict qualitatively the distributions of domains from the values of α_1^E. Smaller values of α_1^E correspond to more packed domains in the plane of the wafer. The magnitude of P_3^R also tells us how many domains are arranged in the thickness direction of the wafer. Then, using the graphs in Figs. 4 and 5, it is possible to draw a two-dimensional schematic diagram for the evolution of internal domain structures at various values of P_3^R. Fig. 6 shows the schematic distributions of internal domains at the states corresponding to five different values of P_3^R denoted by a, b, c, d, e in the upper graph of Fig. 4(a). The evolutions of domain distributions from (a) to (e) in the figure are, therefore, the sequential evolutions of domains obtained by a positive electric field applied to a negatively poled wafer. The diagrams in Figs. 6(a) and (e) correspond to the poled states in $-x_3$ and $+x_3$ directions, respectively. Fig. 6(c) shows the domain distribution corresponding to zero remanent polarization state, where domain distribution is symmetrical with respect to the plane of the wafer. Fig. 6(b) corresponds to the state of minimum α_1^E, where domains are packed most densely in the (x_1, x_2) plane of the wafer. On the other hand, domains are more densely packed in the wafer plane in Fig. 6(c) than in Fig. 6(d), as expected by the larger value of α_1^E in Fig. 6(d) than in Fig. 6(c).

In Fig. 5(a), it is shown that the pyroelectric coefficient p_3^σ depends linearly on the remanent polarization P_3^R for both directions of electric fields. It was also discussed that the

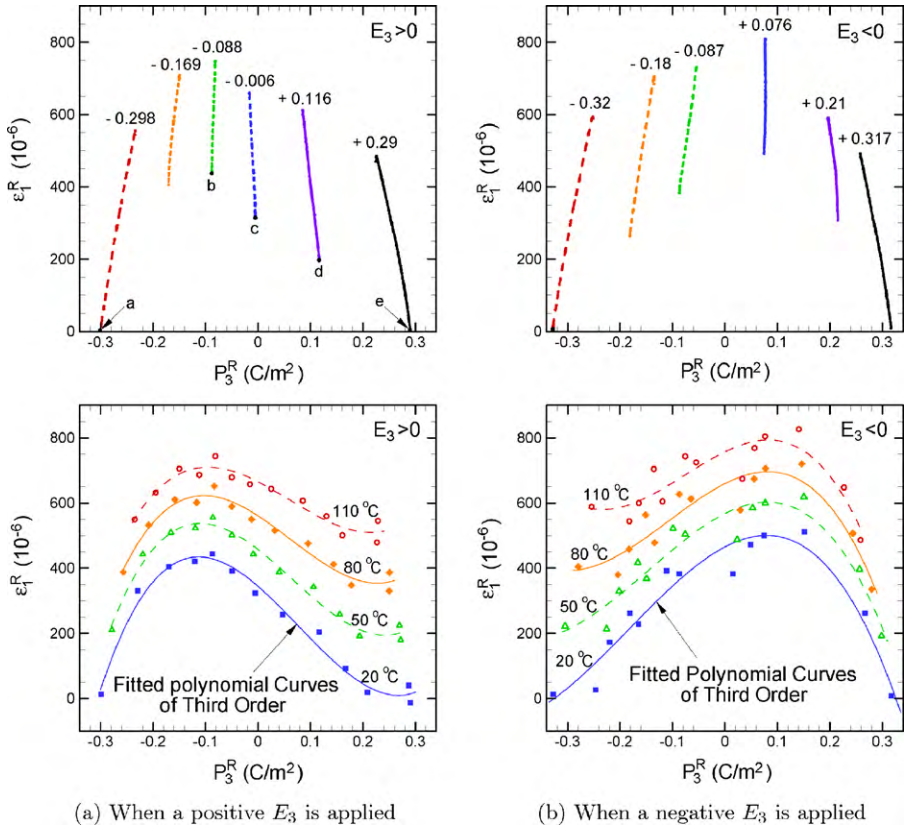

(a) When a positive E_3 is applied (b) When a negative E_3 is applied

Fig. 4. Remanent in-plane strain ε_1^R versus remanent polarization in thickness direction P_3^R plots at various values of reference remanent polarization P_3^{R0} (upper plots) and at four different temperatures (lower plots). A positive electric field is used in (a) and a negative electric field in (b), to reach the initial states for temperature experiments from 20 °C to 110 °C.

positive and negative values of p_3^σ at $P_3^R = 0$ are due to domain switching during temperature increase. Without switching, p_3^σ should stay at zero during the temperature change. The two fitted straight lines for positive and negative electric field cases are parallel to each other and the difference in p_3^σ at constant P_3^R is constant for all values of P_3^R. Neglecting the difference in p_3^σ and fitting all data by one straight line, we get another parallel straight line passing through the origin $(p_3^\sigma, P_3^R) = (0, 0)$. The fitted straight line for all data at 20 °C is shown and designated as 20 °C in Fig. 7(a). Similar fitting can be made for other temperatures and three more fitted straight lines for the data at 50 °C, 80 °C and 110 °C are drawn in Fig. 7(a). Since the magnitude of P_3^R decreases with temperature increase, the magnitude of the slope of the fitted straight line get bigger with temperature rise, as shown in the figure. From the linear relations between p_3^σ and P_3^R, it is useful to express the

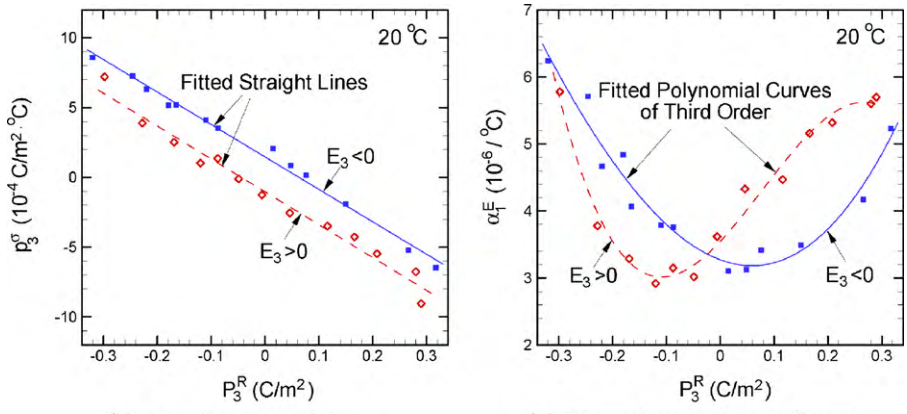

(a) Pyroelectric coefficient (b) Thermal expansion coefficient

Fig. 5. Variations of (a) pyroelectric coefficients p_3^σ and (b) in-plane thermal expansion coefficient α_1^E over remanent polarization P_3^R at 20 °C. The former plots are fitted by straight lines and the latter by polynomial curves of third order. The positive and negative electric fields mean that the initial states for temperature experiments are obtained by a positive or negative electric field, respectively.

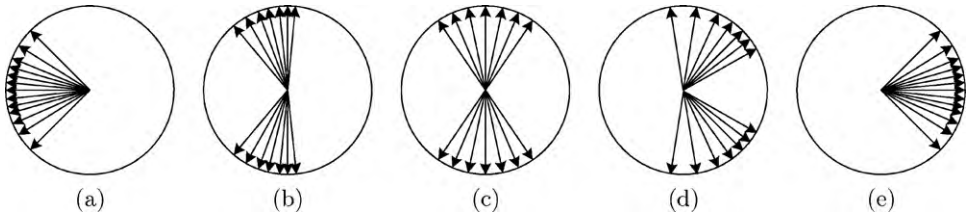

Fig. 6. Schematic domain distributions at the states corresponding to various values of P_3^R obtained by a positive electric field, (a) $P_3^R = -P_3^{R,sat}$, (b) $-P_3^{R,sat} < P_3^R < 0$, (c) $P_3^R = 0$, (d) $0 < P_3^R < +P_3^{R,sat}$, and (e) $P_3^R = +P_3^{R,sat}$. Each figure here corresponds to the state denoted by a, b, c, d and e in Fig. 4(a), respectively.

pyroelectric coefficient p_3^σ as a function of remanent polarization P_3^R by

$$\hat{p}_3^\sigma(P_3^R, \theta) = p_3^{\sigma,sat} \frac{P_3^R}{\hat{P}_3^{R,sat}(\theta)}, \tag{1}$$

where $p_3^{\sigma,sat}(<0)$ is the magnitude of pyroelectric coefficient in thickness direction at the saturated (or poled) state in the tested range of temperature and $\hat{P}_3^{R,sat}(\theta)$ is the magnitude of P_3^R at the saturated state and temperature θ. $\hat{P}_3^{R,sat}(\theta)$ can be given as a function of temperature θ by

$$\hat{P}_3^{R,sat}(\theta) = p_3^{\sigma,sat}(\theta - \theta_0) + P_3^{R0,sat}, \tag{2}$$

where $P_3^{R0,sat}$ is the saturated remanent polarization at the positively poled state and $\theta = \theta_0$. It was observed in Kim et al. [8] that the value of $P_3^{R,sat}$ for the same PZT wafer decreases linearly from $+0.31\,\mathrm{C\,m^{-2}}$ at 20 °C to $+0.25\,\mathrm{C\,m^{-2}}$ at 110 °C at the positively poled state. This gives that $P_3^{R0,sat} = +0.31\,\mathrm{C\,m^{-2}}$ at the positively poled state and $p_3^{\sigma,sat} = -6.8 \times 10^{-4}\,\mathrm{C\,m^{-2}\,°C^{-1}}$ in the tested temperature range. From the fitted straight line in Fig. 7(a), the estimated value of $p_3^{\sigma,sat}$ at 20 °C and $P_3^{R0,sat} = +0.31\,\mathrm{C\,m^{-2}}$ is about $-7.2 \times 10^{-4}\,\mathrm{C\,m^{-2}\,°C^{-1}}$, which gives a negligible 5% error.

It is shown in Fig. 5(b) that the in-plane thermal expansion coefficient α_1^E has an asymmetric distribution over P_3^R for both loading directions of electric field. However, drawing the α_1^E curve over remanent in-plane strain ε_1^R, it is found that α_1^E has the same linear relation with ε_1^R for both directions of electric field. The linear relation is fitted well by a straight line for all measured data at each temperature in Fig. 7(b). The equation of the fitted straight lines can be given by

$$\hat{\alpha}_1^E(\varepsilon_1^R, \theta) = (\alpha_1^{E,m} - \alpha_1^{E,sat}) \frac{\varepsilon_1^R - \hat{\varepsilon}_1^{R,sat}(\theta)}{\hat{\varepsilon}_1^{R,m}(\theta) - \hat{\varepsilon}_1^{R,sat}(\theta)} + \alpha_1^{E,sat}, \tag{3}$$

where $\alpha_1^{E,sat}$ is the in-plane thermal expansion coefficient at the saturated state and $\alpha_1^{E,m}$ is the value of α_1^E at a state near the state of minimum thermal expansion coefficient. Remember that the independent variable ε_1^R in Eq. (3) is an in-plane remanent strain over the reference configuration of the poled (or saturated) state at the reference temperature θ_0. Since the value of α_1^E remains constant during a pure temperature change between 20 °C and 110 °C, the in-plane remanent strains $\hat{\varepsilon}_1^{R,m}(\theta)$ and $\hat{\varepsilon}_1^{R,sat}(\theta)$ at the minimum thermal expansion state and the satuarted state are given, respectively, by

$$\begin{aligned} \hat{\varepsilon}_1^{R,m}(\theta) &= \alpha_1^{E,m}(\theta - \theta_0) + \varepsilon_1^{R0,m}, \\ \hat{\varepsilon}_1^{R,sat}(\theta) &= \alpha_1^{E,sat}(\theta - \theta_0) + \varepsilon_1^{R0,sat}, \end{aligned} \tag{4}$$

where $\varepsilon_1^{R0,m}$ and $\varepsilon_1^{R0,sat}$ are the in-plane remanent strains at the reference temperature θ_0 and at the minimum thermal expansion state and the satuarted state, respectively. Therefore, in order to evaluate α_1^E for given ε_1^R and θ in Eq. (3), it is necessary to measure $\alpha_1^{E,sat}$, $\varepsilon_1^{R0,sat}$ at the saturated state and $\alpha_1^{E,m}$, $\varepsilon_1^{R0,m}$ at a state close to the state of minimum thermal expansion coefficient. Since the reference configuration for strain measures is the negatively (or positively) poled state at $\theta = \theta_0$, the value of ε_1^{R0} at the poled states is zero, i.e., $\varepsilon_1^{R0,sat} = 0$.

The α_1^E versus ε_1^R relations in Fig. 7(b) at various temperatures are linear independent of the directions of the electric fields used to obtain the initial states for temperature

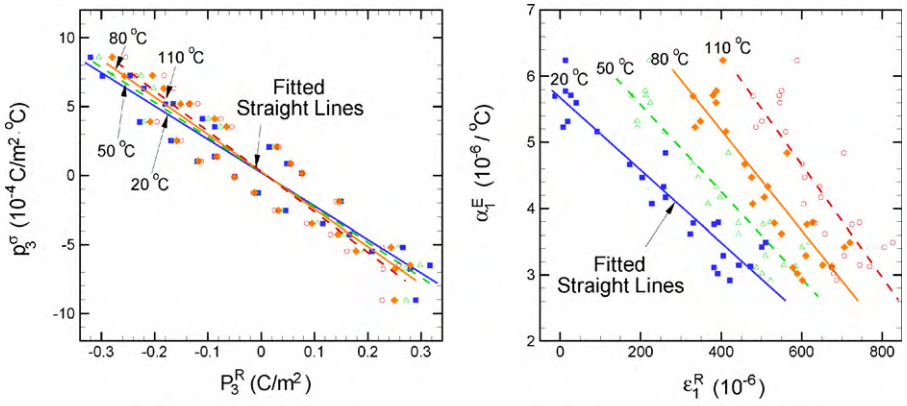

(a) Pyroelectric coefficient (b) Thermal expansion coefficient

Fig. 7. Fitted straight lines of (a) pyroelectric coefficient p_3^σ over remanent polarization P_3^R and (b) thermal expansion coefficient α_1^E over remanent in-plane strain ε_1^R at four different temperatures.

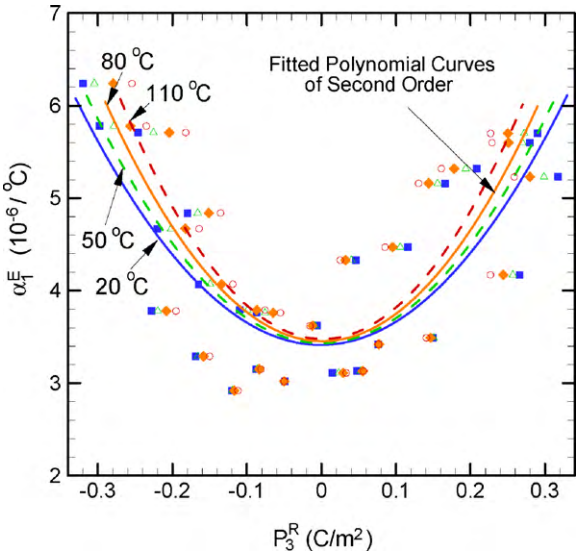

Fig. 8. Fitted second order polynomial curves of thermal expansion coefficient α_1^E over remanent polarization P_3^R at four different temperatures.

experiments, whereas the α_1^E versus P_3^R relations in Fig. 5(b) are asymmetric depending on the directions of electric field. Sometimes it may be useful to evaluate the approximate value of α_1^E by P_3^R, not by ε_1^R. Neglecting the error of about 20%, all plotted data in Fig. 5(b) can be fitted by a polynomial curve of second order, which is shown in Fig. 8 and designated as 20 °C. The fitted second order curve is symmetric with respect to zero polarization vertical line. Similar fittings for the measured data at other temperatures also give other fitted polynomial curves of second order, which are drawn and designated as 50 °C, 80 °C, 110 °C in Fig. 8. Since the magnitude of P_3^R decreases with temperature increase, the fitted second order curves get narrower with temperature increase, as shown in the figure. The equation of the fitted second order polynomial curves in Fig. 8 can be given by

$$\hat{\alpha}_1^E(P_3^R,\theta) = (\alpha_1^{E,sat} - \alpha_1^{E,0})\left(\frac{P_3^R}{\hat{P}_3^{R,sat}(\theta)}\right)^2 + \alpha_1^{E,0}, \quad (5)$$

where $\alpha_1^{E,sat}$ and $\alpha_1^{E,0}$ are the in-plane thermal expansion coefficients at the saturated state and the state of zero remanent polarization, respectively. The saturated remanent polarization $\hat{P}_3^{R,sat}(\theta)$ at temperature θ is given by Eq. (2). From the fitted curves in Fig. 8, it is estimated that $\alpha_1^{E,sat} = 5.75 \times 10^{-6}\,°\mathrm{C}^{-1}$ and $\alpha_1^{E,0} = 3.45 \times 10^{-6}\,°\mathrm{C}^{-1}$. The values of $\alpha_1^{E,m}$ and $\varepsilon_1^{R0,m}$ in Eqs. (3) and (4) can be obtained approximately at the state of zero remanent polarization in Fig. 8. Then, we get $\alpha_1^{E,m} \approx \alpha_1^{E,0} = 3.45 \times 10^{-6}\,°\mathrm{C}^{-1}$ and $\varepsilon_1^{R0,m} \approx \varepsilon_1^{R0,0} = 410 \times 10^{-6}$.

4. Conclusions

A commercially available PZT wafer that is poled in the $-x_3$ (or $+x_3$) thickness direction is subjected to various magnitudes of constant positive (or negative) electric field in the $+x_3$ (or $-x_3$) direction at the reference temperature $\theta_0 = 20$ °C. After reaching a certain value of remanent polarization P_3^R, the electric field loading is stopped and the temperature of wafer is increased up to 110 °C under no electric field. During the pure temperature increase, the variations of remanent polarization P_3^R and remanent in-plane strain ε_1^R are measured. From the measurements, it is found that the pyroelectric coefficient p_3^σ at constant stress and the in-plane thermal expansion coefficient α_1^E remain constant in the tested range of temperature. The variations of ε_1^R over P_3^R are not symmetric with respect to zero polarization vertical line, and they depend on the direction of electric field used to obtain the initial reference remanent polarization.

The evaluated p_3^σ and α_1^E are plotted over remanent polarization P_3^R at $\theta_0 = 20$ °C. It was shown that the pyroelectric coefficient has a linear dependency on remanent polarization and it was well fitted by a straight line. The slopes of the fitted straight lines were the same for both loading directions of electric field. The value of pyroelectric coefficient measured at $P_3^{R0} = 0$ was observed to be positive for negative electric field case but it was negative of the same magnitude for positive electric field case. The nonzero values of pyroelectric coefficient at $P_3^{R0} = 0$ indicate that domain switching does occur during the temperature increase at $P_3^{R0} = 0$. More interestingly, the direction of domain switching depends on the direction of electric field: it occurs in the negative direction for positive electric field case but in the positive direction for negative electric field case. Neglecting the small error due to domain switching, the pyroelectric coefficient could be expressed as a linear function of remanent polarization. The variations of in-plane thermal expansion coefficient over remanent polarization also depended on the directions of electric field. Neglecting the relatively small error of about 20%, the in-plane thermal expansion coefficient could be fitted relatively well by polynomial curves of second order and given as a quadratic function of remanent polarization. The thermal expansion coefficient was also plotted over remanent in-plane strain and it was well expressed as a linear function of remanent in-plane strain.

Acknowledgement

This work was supported by the Seoul R&BD Program (10890).

References

[1] M. Selten, G.A. Schneider, V. Knoblauch, R.M. McMeeking, On the evolution of the linear material properties of PZT during loading history—an experimental study, Int. J. Solids Struct. 42 (2005) 3953–3966.
[2] Q.D. Liu, J.E. Huber, State dependent linear moduli in ferroelectrics, Int. J. Solids Struct. 44 (2007) 5635–5650.
[3] D. Zhou, M. Kamlah, Room-temperature creep of soft PZT under static electrical and compressive stress loading, Acta Mater. 54 (2006) 1389–1396.
[4] Q.D. Liu, J.E. Huber, Creep in ferroelectrics due to unipolar electrical loading, J. Eur. Ceram. Soc. 26 (2006) 2799–2806.
[5] S.J. Kim, C.H. Lee, Creep behavior of a poled PZT wafer under longitudinal tensile stress and through thickness electric field, Int. J. Solids Struct. 46 (2009) 716–725.

[6] T. Sakai, H. Kawamoto, Durability properties of piezoelectric stack actuator, Jpn. J. Appl. Phys. 37 (1998) 5338–5341.
[7] J.H. Kim, C.H. Lee, S. Lee, S.J. Lee, S.J. Kim, Time-dependent behavior of a lead titanate zirconate wafer under constant electric fields at high temperatures, Jpn. J. App. Phys. 48 (2009) 101404.
[8] S.J. Kim, J.H. Kim, C.H. Lee, Domain switching and creep behavior of a poled PZT wafer under through-thickness electric fields at high temperatures, Acta Mater. 58 (2010) 2237–2249.
[9] F. Jona, G. Shirane, Ferroelectric Crystals, Pergamon Press, 1962.